Available online at www.sciencedirect.com
SCIENCE DIRECT
Journal of Catalysis 239 (2006) 313–325
JOURNAL OF CATALYSIS
www.elsevier.com/locate/jcat

Carbon-supported ruthenium catalysts for NH_3 synthesis doped with caesium nitrate: Activation process, working state of Cs–Ru/C

Wioletta Raróg-Pilecka [a], Elżbieta Miśkiewicz [a], Sławomir Jodzis [a], Jan Petryk [a], Dariusz Łomot [b], Zbigniew Kaszkur [b], Zbigniew Karpiński [b], Zbigniew Kowalczyk [a,*]

[a] *Warsaw University of Technology, Faculty of Chemistry, Noakowskiego 3, 00-664 Warsaw, Poland*
[b] *Institute of Physical Chemistry of the Polish Academy of Sciences, Kasprzaka 44/52, 01-224 Warsaw, Poland*

Received 17 January 2006; revised 31 January 2006; accepted 31 January 2006

Available online 10 March 2006

Abstract

The process of an active Cs–Ru/carbon catalyst formation (reduction) was studied in detail, using graphitised carbons as supports for ruthenium and caesium nitrate as a promoter precursor. In situ XRD and TPR-MS techniques were applied to monitor the changes in the specimens when heating in H_2 and $H_2 + Ar$ mixtures, respectively. The postactivation state of the catalysts (i.e., the state corresponding to ammonia synthesis conditions) was characterised chemically via interaction of the reduced samples with water vapour at 50 °C (H_2 evolution) and also via interaction with oxygen at 0 °C. These experiments were supplemented with those of ammonia synthesis. Ruthenium was shown to facilitate the decomposition of caesium nitrate; whereas the Ru-free $CsNO_3$/C reference materials are stable in a flowing $H_2 + Ar$ mixture up to about 400 °C, the $CsNO_3$ decomposition starts at 100–120 °C for the $CsNO_3$–Ru/C catalysts (XRD, TPR-MS) and proceeds via a $CsOH{\cdot}H_2O$-intermediate product that turns into an amorphous species at elevated temperatures, as indicated by XRD. Characterisation studies of the postactivation catalysts showed that caesium is partially reduced during operations and reacts with oxygen (O_2 consumption) and water vapour (H_2 evolution). The degree of promoter reduction resulting from H_2 liberation varies from 0.25 to 0.45, depending on the Cs loading, Ru loading, and kind of carbon. Combining the O_2 consumption and H_2 evolution data suggests that a substoichiometric oxide (Cs_xO_y; $x/y = 2.7$–3.6) exists on the catalyst surface rather than $Cs^0 + CsOH$. High activities (TOFs) of the optimally promoted Cs–Ru/C systems in ammonia synthesis (63 bar, 370 and 400 °C) were ascribed to the strong promotional effect of partly reduced caesium (Cs_xO_y) covering the Ru surface. A peculiar S-like shape of the TOF trace versus Cs loading is suggested to be a consequence of the promoter distribution between the carbon surface and surface of ruthenium. Clearly, the trend in TOF reflects that in Ru coverage by the Cs_xO_y groups, the latter being controlled by the heats of Cs_xO_y adsorption on ruthenium and on carbon, respectively.

Keywords: Ammonia synthesis; Ruthenium catalysts; Graphitised carbon support; Caesium promoter; Activation process; Promoter active state

1. Introduction

Since the work of Haber and Bosch, the commercial process of NH_3 synthesis has been performed over iron catalysts manufactured by fusion of magnetite with small amounts of additives (e.g., K_2O, Al_2O_3, CaO) [1]. Such catalysts are stable at even high temperatures [1,2], but their activity drops significantly with decreasing total pressure [3] and with increasing ammonia concentration in the gas [4]. Consequently, efforts have been made to improve the activity of conventional Fe catalysts [5–7] or to develop a new system that would be able to operate effectively under the low-pressure conditions.

Among noniron catalysts (i.e., ternary nitrides [8–13], cobalt on carbon [14,15], ruthenium deposited on various carriers [16–52]), the Ru-based systems are the most prospective, particularly when carbon is used as a substrate for the metal. Over the last decade, ruthenium catalysts supported on thermally modified, partly graphitised carbon have been used successfully in several large-scale ammonia plants operating under the Kellog

* Corresponding author.
E-mail address: zbyko@ch.pw.edu.pl (Z. Kowalczyk).

0021-9517/$ – see front matter
doi:10.1016/j.jcat.2006.01.035

(Kellog Brown & Root) license [53,54]. Although the unpromoted Ru/C materials are rather inactive in NH_3 synthesis [38], they become extremely active on promotion with barium or alkali, especially caesium [36,37,43,55,56]. At high conversions, corresponding to the final bed of an industrial reactor, the Ru/C catalysts doped with caesium are more active than those doped with barium [57], and both are significantly more active than the magnetite-based catalysts.

Usually, caesium nitrate is used as a Cs precursor for the Cs–Ru/C catalyst preparation. Before NH_3 synthesis, the $CsNO_3$–Ru/C systems are activated in hydrogen or a $H_2 + N_2$ mixture, leading to Ru surface reduction and Cs precursor decomposition. To date, the working state of Cs–Ru/C or, more precisely, the state of caesium (chemical form(s)) and its location, as well as the promoting mechanism, have not been univocally explained. It is commonly believed that alkalis act as electronic promoters; that is, promotion proceeds via electron transfer from the alkali to the metal surface (Ru, Fe). An electron-rich surface is then more active for nitrogen dissociative adsorption (the rate-determining step of NH_3 synthesis) [58–61], and NH_x species, including adsorbed ammonia, are destabilised [62–66], resulting in more free active sites on the metal surface and thus increasing its activity [62,63]. According to the foregoing concepts, the effect of caesium is closely related to the state of the promoter when operating; the more reduced the Cs promoter, the stronger the expected promotional effect.

Extensive studies of the Cs-doped Ru catalysts supported on carbon [55,56] and magnesia [67] have revealed that the catalytic properties of ruthenium surfaces in ammonia synthesis are strongly dependent on the choice of the support material (MgO, C). The NH_3 synthesis rates (TOF) over the former system (Cs–Ru/C) were significantly higher than those over the latter (Cs–Ru/MgO), although the dispersions were close to one another. Thus, one may suppose that the state of caesium in Ru/C is different from that in Ru/MgO. Tennison suggested [68] that the more probable form of the alkali in ruthenium/carbon is a $M^+\cdots C^-$ charge-transfer complex in which reduction of the promoter salt is driven by the high heat of the carbon–alkali complex formation. Support for such a hypothesis comes from the thermodynamic calculations [68]. The reduction of caesium nitrate (carbonate) in hydrogen should occur even at high water vapour pressures and even when assuming a relatively low heat of adsorption for the metal on the graphite surface. Indeed, recent XPS [69,70] and UPS [69] studies of the carbon-based Ru catalysts demonstrate that the alkali promoter (Cs, K) is strongly reduced under ammonia synthesis conditions (a substoichiometric alkali + O adlayer on both the graphitic support and Ru particles [69], a partly metallic state of the alkali [70]). In contrast to the foregoing, the groups of Aika [71], Guan [72], and Forni [73] claim that the main phase of the alkali is hydroxide when operating, both for Cs–Ru/MgO [27] and Cs–Ru/C [27,72,73].

The purpose of this work was to study in detail the process of an active Cs–Ru/C catalyst formation using $CsNO_3$ as an alkali precursor, and to quantitatively characterise the resultant state of the Cs promoter, that is, the state corresponding to the ammonia synthesis conditions. Studies of activation were performed in a XRD camera equipped with a position-sensitive detector and, in addition, in a conventional TPR setup equipped with a mass spectrometer as an analytical tool. The active state of the catalysts was characterised chemically via interaction of the reduced samples with water vapour and, incidentally, via interaction with oxygen. The former reaction (with water vapour) was expected to be a source of hydrogen if Cs was in its reduced form; neither CsOH nor Cs_2O can produce H_2 when contacting with H_2O. Hence the amount of hydrogen evolved to the gas phase would be a precise measure of the degree of promoter reduction. Oxygen in turn may be consumed by the ruthenium surface (chemisorption) and Cs_xO_y species including Cs^0 but is inert to the alkali hydroxides. All of the above characterisation experiments were supplemented with those of high-pressure ammonia synthesis. Namely, the effect of Cs loading and that of Ru loading on the activity were examined to check whether the promoter state is correlated with the catalytic properties of the system.

2. Experimental

2.1. Carbon supports, Cs–Ru/C catalysts

Three carbon materials, marked throughout the text as A, B_1, and B_2 were used as supports for the catalysts preparation. Carbon A was obtained via high-temperature heating (1900 °C, 2 h, helium atmosphere [74]) commercial activated carbon RO 08 supplied by the Norit B.V. Company. The other two materials (B_1, B_2) were derived from GF 45 starting carbon (Norit B.V.) by its two-step modification consisting in high-temperature treatment (1900 °C, 2 h, He) and subsequent gasification in a CO_2 stream at about 850 °C up to 24.6% mass loss (B_1) or, alternatively, by gasification with a H_2O:Ar = 1:1 mixture (B_2) to 28% loss of mass. Finally, the materials were washed with distilled water to remove fines and dried in air at 120 °C for 24 h. Nitrogen physisorption and mercury porosimetry studies have shown (see Table 1) that carbons B_1 and B_2 expose a significantly more developed texture than A.

For Ru/carbon, the supports were impregnated with a THF solution of ruthenium carbonyl (Ru/A) or with acetone solutions of ruthenium chloride (Ru/B_1, Ru/B_2). After drying in air at 60 °C, the samples were reduced in flowing hydrogen of high purity (99.9999%), first at 150 °C for 24 h and then at 350 °C for 24 h, followed by passivation with air pulses introduced to an Ar stream. Typically, the Ru content was kept constant (9.1 wt%). In the case of high metal loading

Table 1
Textural parameters of the carbon supports; S_{BET}—BET surface area; S_{Hg}, V_{Hg}, V_{mHg}—surface area, total volume of pores and volume of pores in the range of 3–100 nm, as determined by mercury porosimetry

Carbon material	S_{BET} (m^2/g)	S_{Hg} (m^2/g)	V_{Hg} (cm^3/g)	V_{mHg} (cm^3/g)
A	66	60	0.61	0.21
B_1	1034	192	0.47	0.295
B_2	1257	278	0.70	0.48

(20 wt%), the impregnation–reduction–passivation procedure was repeated several times.

Caesium nitrate (the Cs precursor) was introduced to the Ru/carbon systems through impregnation from aqueous solutions, followed by drying the samples in air at 90 °C for 24 h. To easily distinguish among the catalysts prepared, all of the samples were labelled with unified symbols that specified in sequence; the Cs loading [expressed in $mmol_{Cs}/g_{C+Ru}$], the Ru loading (wt%), and the kind of carbon (A, B_1, B_2), for example, Cs0.36–Ru9.1/B_1.

2.2. Studies of catalyst activation

2.2.1. XRD

The examinations were performed in a setup that enabled studying the specimens under controlled temperature and gas composition. The powdered sample was spread on porous glass and placed on the holder of a home-built XRD camera, as described previously [75]. The camera was positioned on an INEL goniometer equipped with a CPS-120 position-sensitive detector (PSD) that allowed simultaneous recording of the diffraction pattern within a wide range of diffraction angles ($2\Theta = 120°$). The PSD operated with 4096 channels and provided resolution of ∼0.03°/channel. Cu-K_α radiation with a primary beam flat graphite monochromator was applied. The measurements were carried out in a hydrogen stream (99.9999% purity); the temperature was increased linearly at a rate of 3 °C/min up to about 450 °C, and the flow rate of a gas stream was kept constant at 20 mL/min. A sequence of the XRD patterns was recorded at intervals of 5 min with counting time of 3 min for each pattern. Data collection was controlled by a computer program.

2.2.2. TPR-MS

The temperature-programmed reduction (activation) experiments were carried out in a tubular flow reactor using 6% H_2/Ar or 80% H_2/Ar mixtures (40 mL/min), preliminarily purified from traces of oxygen and water vapour by passing over the 15% Mn/SiO_2 and drying traps. The reactor outlet was connected via a T-union to the sampling valve of a Dycor Ametek MA 200 quadrupole mass spectrometer that enabled simultaneous recording of 12 mass signals. The temperature of the reactor was increased up to 430 °C at a ramp rate of 10 °C/min, at which point the reduction of the sample was continued. To determine the changes in relative amounts of various species evolving to the gas phase, the spectra thus obtained were elaborated in terms of standard spectra of respective compounds.

2.3. Characterisation studies of the activated catalysts

2.3.1. Interaction with water vapour

Studies of interaction between the reduced catalysts and water vapour were performed in the setup described above (TPR-MS), using the following procedure. After the reduction had been completed (430 °C, 16 h, 80% H_2/Ar), the sample was flushed with argon (40 mL/min) at 430 °C for 30 min to remove hydrogen, and then cooled in flowing argon. Subsequently, the Ar stream was replaced with an H_2O/Ar mixture obtained by passing argon through a bubbler filled with redistilled water. Both H_2O and H_2 were monitored with a mass spectrometer after switching from argon to H_2O/Ar; the latter signal (H_2) was used for determining the total amount of hydrogen desorbed to the gas. All of the experiments were performed under fixed conditions; the temperature of the bubbler was 40 °C (7% H_2O in a 40-mL/min Ar stream) and that of the reactor was 50 °C, whereas the mass of the catalyst (0.2–0.63 mm particles) was 0.15 g_{C+Ru}. To avoid water condensation in the setup, all of the relevant tubing, stopcocks, and connections were heated.

2.3.2. Interaction with oxygen

The examinations were carried out in a conventional, fully automated temperature-programmed setup (manufactured by Technical University of Łódź), equipped with a U-tube reactor and a thermal conductivity dectector cell [56]. The sample was reduced in a H_2:He = 80:20 mixture (40 mL/min) at 430 °C for 16 h and, after flushing with helium at 430 °C (40 mL/min for 30 min), cooled in a He stream. Then the oxygen uptake was measured at 0 °C by adding O_2 pulses (6.25 μmol) to flowing helium. Both caesium-free and Cs-doped catalysts were tested. The data obtained for the unpromoted samples were used for calculating the ruthenium dispersion, expressed as the fraction exposed (FE) and average particle diameter (d). The details of such calculations have been provided elsewhere [39]. The amount of oxygen consumed by the promoter in Cs–Ru/carbon was assumed to be the difference between the overall O_2 uptake (corresponding to Cs–Ru/C) and that determined for the unpromoted material. As shown previously [47,53], Ru dispersion remains unchanged on promotion when activation is performed under mild conditions.

2.4. Activity studies

The activity of the catalysts in ammonia synthesis was measured in a flow tubular reactor supplied with a very pure (H_2O < 0.5 ppm) H_2:N_2 = 3:1 mixture. Under steady-state conditions of temperature (400 or 370 °C), pressure (63 bar) and gas flow rate (70 dm^3 [STP]/h), the concentration of ammonia in the stream leaving the catalyst bed (0.15 g_{C+Ru}; 0.2–0.63 mm grain size) was monitored. Consequently, the integral reaction rate (productivity) could be determined. Some experiments with an ammonia-rich inlet stream (8% NH_3, differential measurements) were also performed.

Before kinetic testing, the $CsNO_3$–Ru/C samples were reduced (activated) in a stoichiometric $H_2 + N_2$ mixture at 430 °C for 16 h (p = 1 bar). Hence the activation conditions corresponded to those applied in the characterisation studies: interaction with H_2O or O_2 (see above).

3. Results

3.1. Activation process

Two $CsNO_3$–Ru/carbon samples with the same Ru loading but different supports were examined by in situ XRD; the re-

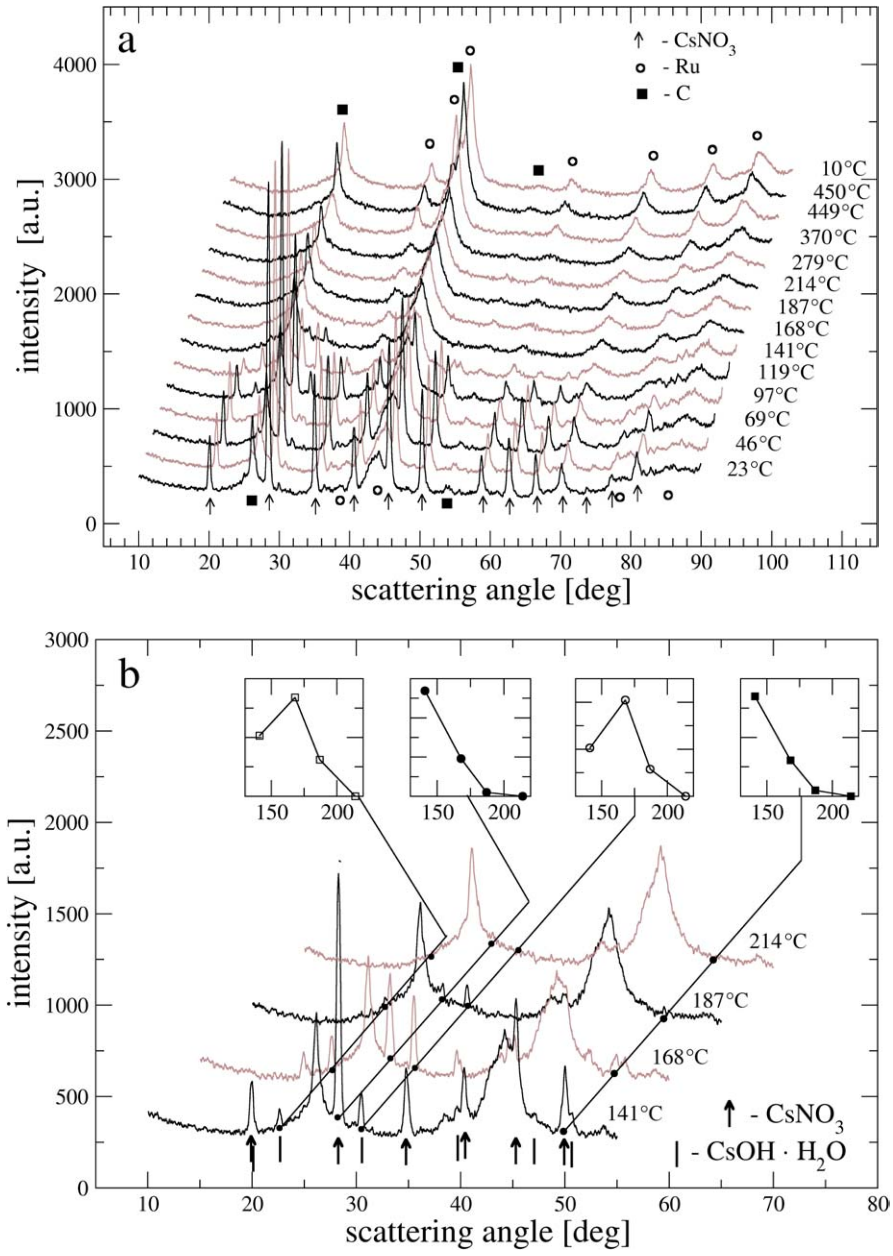

Fig. 1. In situ XRD studies of the $CsNO_3$1.49–Ru9.1/A specimen: (a) pattern evolution with temperature; (b) fragment of the patterns illustrating decomposition of the $CsNO_3$ salt resulting in formation of an intermediate $CsOH{\cdot}H_2O$ phase.

sults are shown in Figs. 1 and 2. Fig. 1 illustrates the changes in the system prepared from low-surface area carbon A, and Fig. 2 shows results for the specimen derived from the B_1 material of more highly developed pore structure.

As shown in Fig. 1a, the XRD pattern of the starting $CsNO_3$–Ru/A sample is rather complex. The distinct reflections of the promoter precursor are accompanied by those of carbon and ruthenium, thus indicating that carbon A is well organised and the metal particles are large. Decomposition of $CsNO_3$ starts at about 120 °C and leads to the formation of crystalline caesium hydroxide ($CsOH{\cdot}H_2O$)-intermediate product, which turns into an amorphous species at elevated temperatures. The highest intensity of the $CsOH{\cdot}H_2O$ reflections is observed at 168 °C (see Fig. 1b). The C(002) peak position corresponding to the postreduction specimen cooled in hydrogen to room temperature is identical to that for the fresh sample. This means that the compound of carbon and caesium (graphite intercalation compound [GIC]) is not formed during the activation process. (GIC formation would be expected to result in an increase of the graphite 002 interplanar distance and, consequently, a shift in the C002 peak position toward smaller diffraction angles.)

In contrast to that of $CsNO_3$–Ru/A, the XRD pattern of the fresh $CsNO_3$–Ru/B_1 specimen is dominated by the presence of the Cs salt (Fig. 2). The reflections of carbon and those of ruthenium are diffuse, with poorly ordered substrate material and small Ru crystallites. Decomposition of caesium nitrate begins at about 120 °C, analogously to $CsNO_3$–Ru/A, and pro-

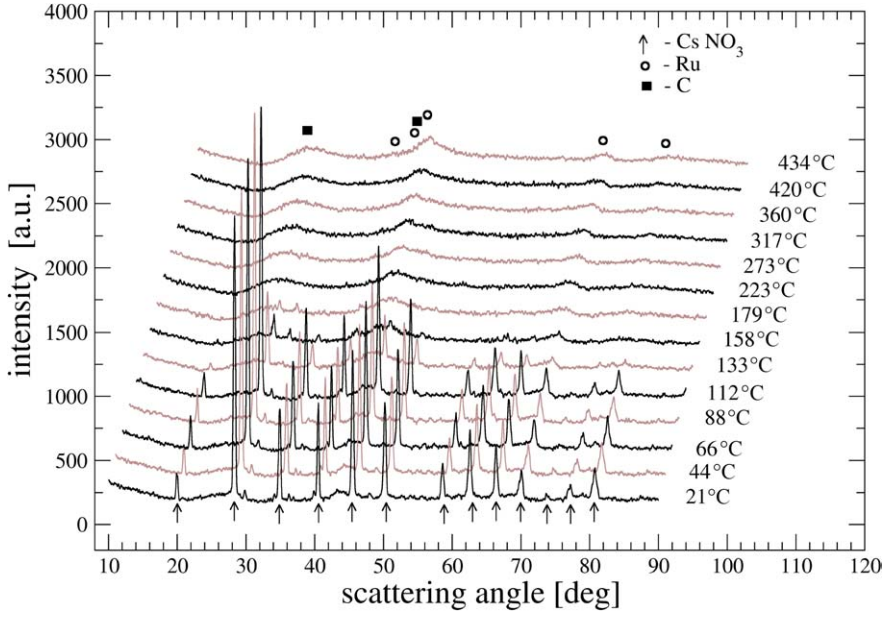

Fig. 2. In situ XRD studies of the $CsNO_3$2.64–Ru9.1/B_1 specimen. Pattern evolution with temperature.

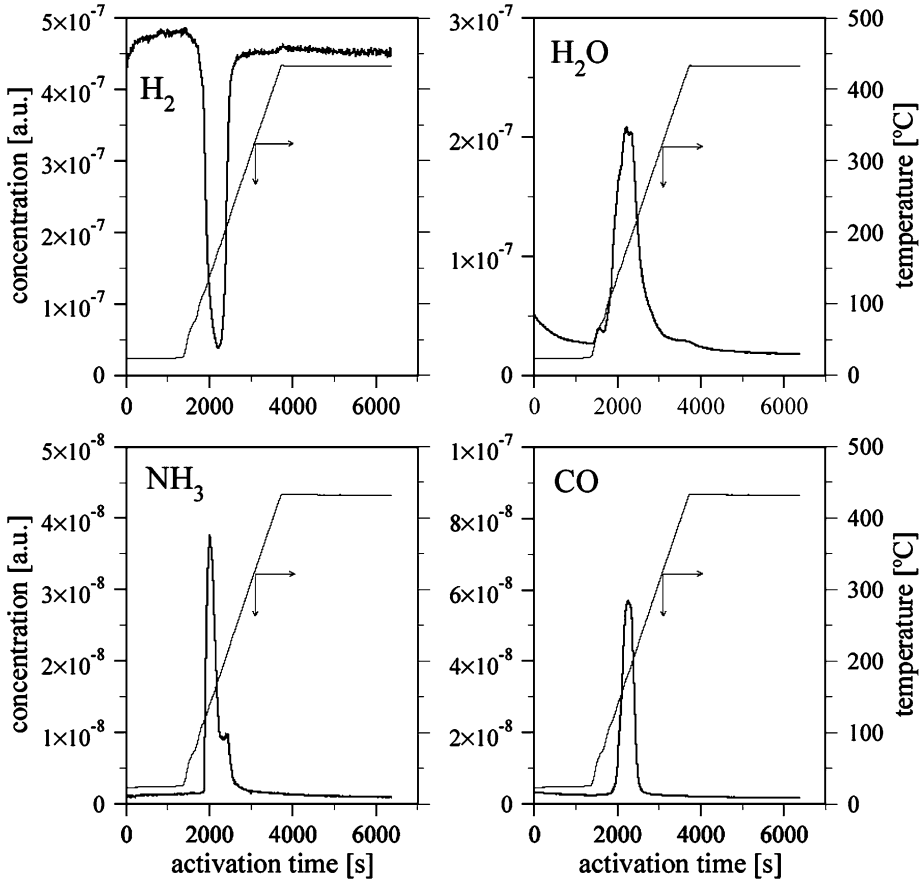

Fig. 3. TPR-MS studies of the $CsNO_3$1.49–Ru9.1/A catalyst: concentrations of the main components in the outlet gas stream (6% H_2/Ar, 40 mL/min) and temperature vs. activation time; the starting sample (0.2585 g) contained 0.1822 g carbon, 0.0182 g Ru and 0.0581 g $CsNO_3$.

ceeds over a narrow range of temperatures (120–180 °C) without any intermediate phases that would be detectable by XRD. The patterns recorded at temperatures above 180 °C are identical to those of the unpromoted Ru/B_1 material (not shown), demonstrating that caesium nitrate is converted to an amorphous species.

The TPR-MS data obtained for the $CsNO_3$–Ru/A and $CsNO_3$–Ru/B_1 catalysts, both activated in a 6% H_2/Ar mix-

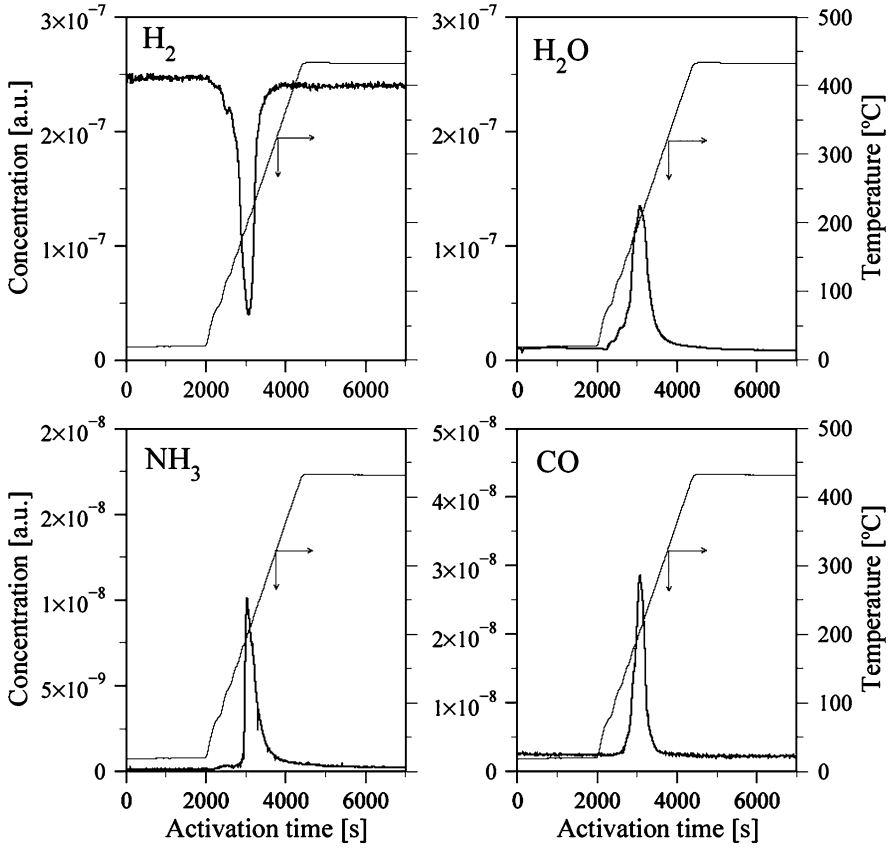

Fig. 4. TPR-MS studies (6% H_2/Ar, 40 mL/min) of the $CsNO_3$2.64–Ru9.1/B_1 catalyst; the starting sample (0.1903 g) contained 0.1201 g carbon (B1), 0.0120 g Ru and 0.0582 g $CsNO_3$.

ture, are shown in Figs. 3 and 4. In these figures the changes in concentrations of the abundant compounds (arbitrary units) and those in temperature are plotted versus time of the experiment. In general, there is no difference between the two samples. Consumption of hydrogen starts at about 100 °C, in accordance with the XRD results presented in Figs. 1 and 2, and is accompanied by the evolution of water vapour, ammonia, and carbon monoxide as the main reaction products. Small amounts of nitrogen, carbon dioxide, and methane were also detected in the effluent gas (not shown in Figs. 3 and 4). Analogous trends in evolution of MS signals were found when the 80% H_2/Ar mixture was used instead of 6% H_2/Ar. In that case, however, the changes in the H_2 and NH_3 concentrations were limited to a slightly narrower temperature range, and hydrogen consumption peaks were, for obvious reasons, significantly less pronounced. The foregoing results demonstrate that nitrate anions in $CsNO_3$ are reduced with hydrogen to mainly ammonia (because the N_2 signal is considerably weaker than the NH_3 signal; see Figs. 3 and 4), in agreement with the literature data reported for $CsNO_3$–Ru/MgO and several model systems [27,76].

To gain better insight into the effect of the presence of ruthenium on caesium nitrate decomposition, the Ru-free reference materials $CsNO_3$/A and $CsNO_3$/B_1 were also evaluated by TPR-MS. In contrast to the ruthenium-containing specimens, these materials proved stable in a 6% H_2/Ar stream up to about 400 °C (Figs. 5 and 6). Furthermore, large amounts of CO_2, N_2O, or both (N_2O and CO_2 being barely distinguishable by MS) were observed in the outlet gas during the activation process. Thus, it is clear that ruthenium facilitates $CsNO_3$ decomposition in hydrogen, most likely via atomic hydrogen formation [71]. The hydrogen atoms adsorbed on the Ru surface spill over the carbon support and, due to high reactivity, interact with the $CsNO_3$ phase even at temperatures as low as 100–120 °C.

3.2. Working state of the Cs–Ru/C systems

3.2.1. Interaction of the reduced catalysts with oxygen

Blank experiments have shown that the carbon supports are totally inert to oxygen. Consequently, the amounts of O_2 consumed by the unpromoted samples may be ascribed solely to the presence of ruthenium in the systems, and those for the Cs-doped catalysts should be ascribed to Ru + Cs. The most relevant results of the studies performed with Ru/carbon and Cs–Ru/carbon specimens are collected in Table 2. The table also includes data obtained for one of the ruthenium-free Cs/carbon materials (Cs/B_1).

As seen in Table 2, Ru dispersion depends strongly on the carbon type (A vs. B_i) or, more precisely, on its texture. A higher surface area of the support (see Table 1) results in a smaller Ru particle size. The effect of loading on the active-phase dispersion seems to be less pronounced; an approximate seven-fold increase in the metal content leads to a two-fold reduction in particle size for both Ru/B_1 and Ru/B_2 (see Table 2).

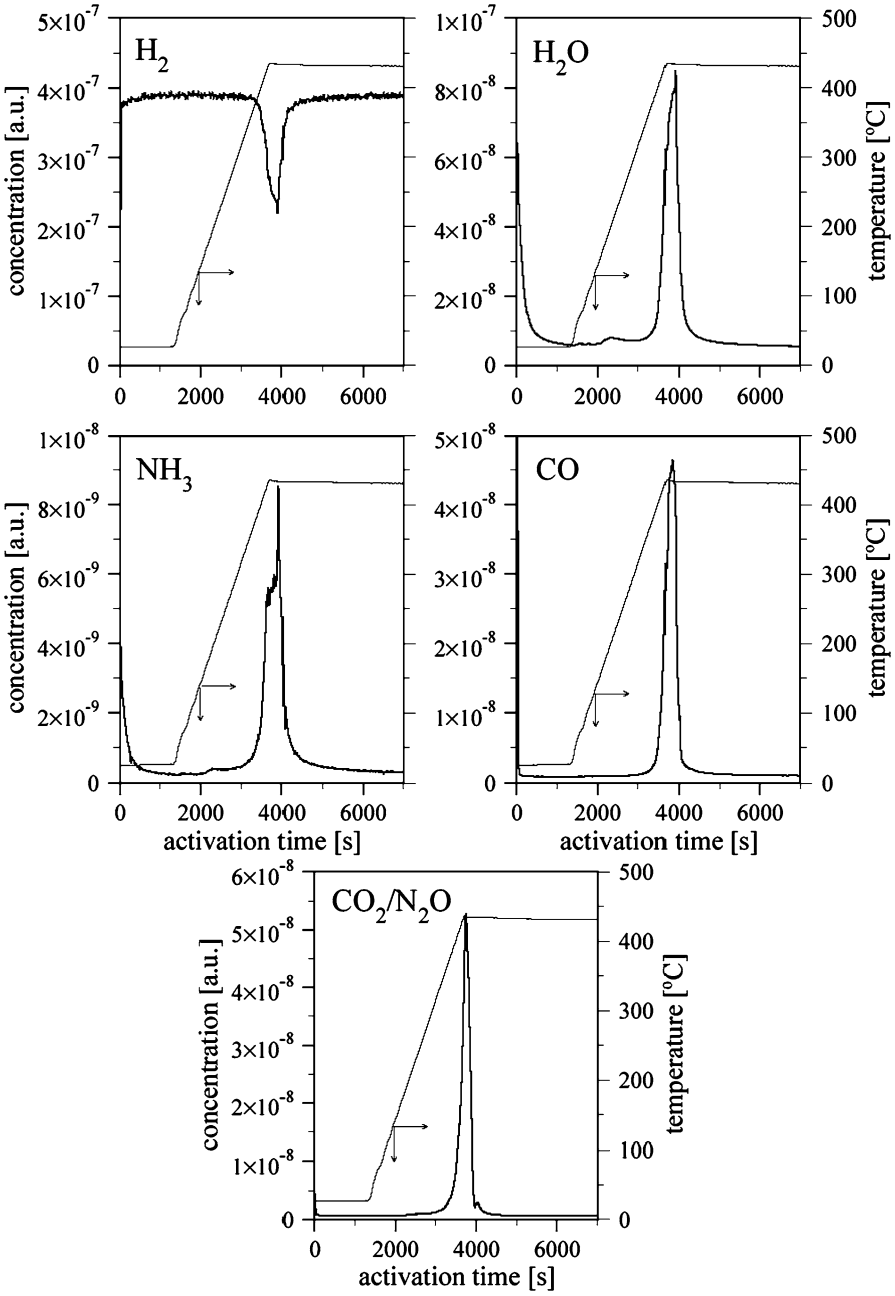

Fig. 5. TPR-MS studies of the Ru-free $CsNO_3$/A sample (6% H_2/Ar); the starting material (0.2332 g) contained 0.0510 g $CsNO_3$.

The amounts of oxygen taken up by the caesium-promoted catalysts are larger than those for the Ru/carbon precursors. In the case of low ruthenium content and high caesium content (Cs3.1–Ru3/B_1), O_2 consumption is dominated by the promoter addition. An oxygen balance performed for that sample as well as for the other samples with high Cs loading shows that about 1 mol of oxygen atoms is used for the neutralisation of 1 mol of caesium. For the sample with a low Cs content (Cs0.33–Ru9.1/B_1), the relative oxygen uptake corresponding to the promoter is significantly greater (O:Cs = 1.76:1).

Oxygen is also reactive to the Cs/B_1 material preliminarily heated in hydrogen. However, the O_2 consumption related to the total number of Cs atoms (O:Cs = 0.6:1; see Table 2) is less than that for the Cs–Ru/B_1 samples. Because the chemical form of caesium in the postoxidation specimens is unknown (Cs may form various oxides, including CsO_2), it is impossible to determine the operating state of the promoter from the O_2 consumption data. Nonetheless, it is that caesium hydroxide is inert to oxygen. So, should caesium nitrate be decomposed exclusively to hydroxide, as has been suggested [71–73], oxygen would be consumed by the ruthenium surface only (Cs–Ru/carbon) and would not be reactive to Cs/carbon. This was not the case, however. A more detailed discussion of the O_2 sorption results is presented later in this paper.

3.2.2. *Interaction of the catalysts with water vapour*

As expected, hydrogen proved to be the only gaseous product of the reaction between water vapour and the catalyst mate-

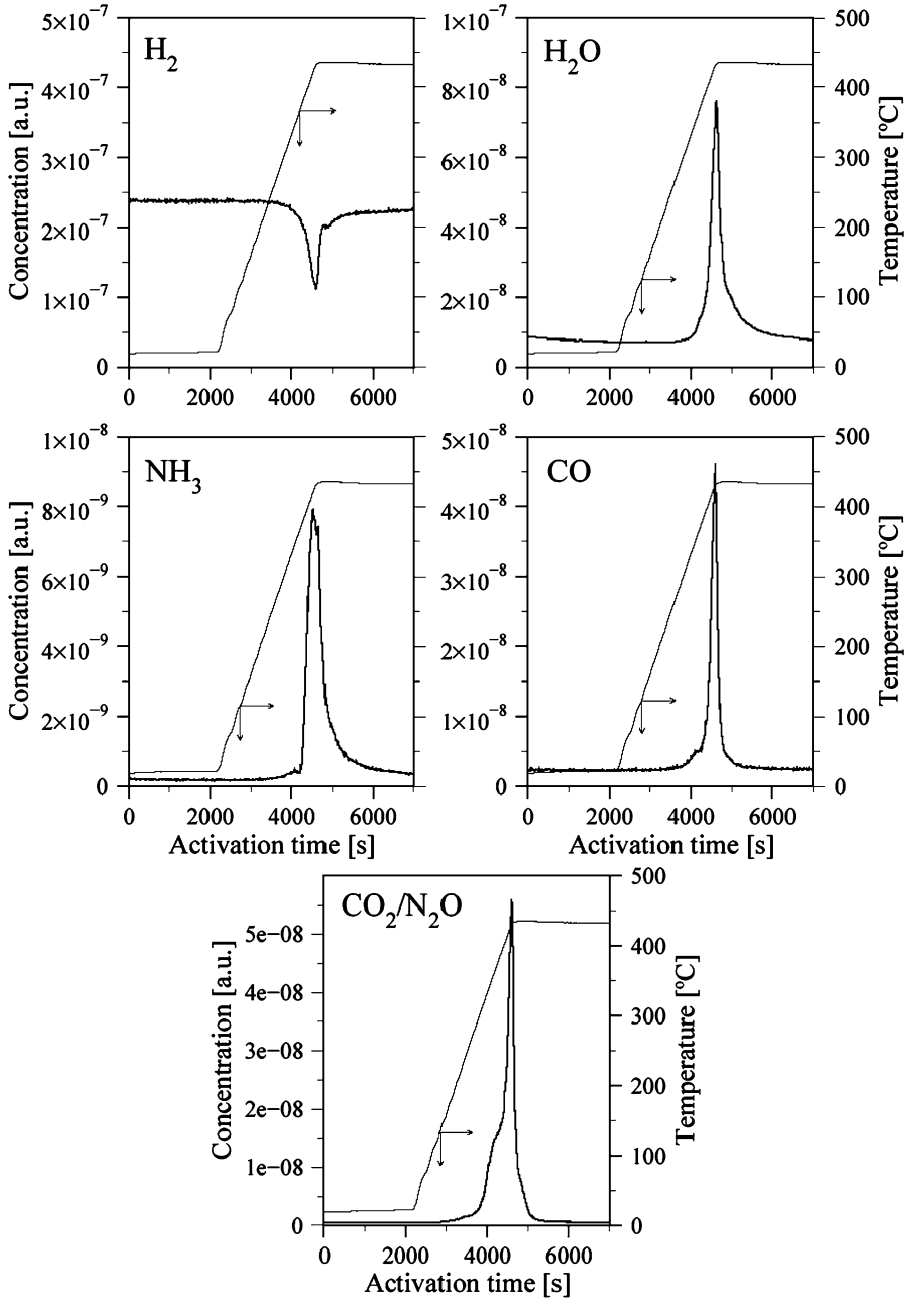

Fig. 6. TPR-MS studies (6% H_2/Ar) of the $CsNO_3/B_1$ sample (0.1610 g) that contained 0.0597 g $CsNO_3$.

rial. A typical MS signal of H_2 evolution, as determined for one of the samples at 50 °C, is shown in Fig. 7. An identical signal was obtained at a slightly higher temperature (70 °C). Therefore, the systematic studies of different catalysts (see below) were performed only at 50 °C.

Fig. 8 illustrates the effect of Cs loading on the hydrogen evolution. All of the catalysts examined in that series of experiments contained 9.1 wt% Ru in relation to (C + Ru), and all were derived from carbon B_1. The amount of hydrogen evolved to the gas phase was determined by integrating the MS-H_2 signals. As shown in Fig. 8, H_2 emission increases systematically with the Cs content, from 15 $\mu mol/g_{C+Ru}$ for the Cs-free material to 580 $\mu mol/g_{C+Ru}$ for the material with the highest caesium content (4.0 $mmol/g_{C+Ru}$). The H_2 emission data were used, after correction (Ru/B_1—15 $\mu mol_{H_2}/g_{C+Ru}$), to determine the number of equivalent Cs^0 atoms (Cs^0_{eq}) responsible for the hydrogen production ($Cs^0 + H_2O = CsOH + (1/2)H_2$) and, consequently, to determine the reduction degree of caesium ($RD = Cs^0_{eq}/Cs_{total}$). The results of such calculations (Fig. 9; trace RD) clearly show that a significant portion of the promoter is reduced during operation. However, whereas the number of Cs^0_{eq} atoms increases monotonically (trace Cs^0 in Fig. 9), the RD parameter decreases slightly with Cs loading, from a value of 0.43 for the lowest Cs content (0.33 $mmol_{Cs}/g_{C+Ru}$) to about 0.28 for the highest Cs content (4.0 $mmol_{Cs}/g_{C+Ru}$).

Table 2
Interaction of the Ru/carbon and Cs–Ru/carbon catalysts with oxygen

Sample	Total O_2 uptake ($\mu mol/g_{C+Ru}$)	O_2 uptake corresponding to caesium (mol_O/mol_{Cs})	FE_{Ru}	d_{Ru} (nm)
Ru9.1/A	80.1	–	0.16	8.4
$Ru3/B_1$	118.3	–	0.73	1.3
$Ru9.1/B_1$	293.3	–	0.59	1.7
$Ru20/B_1$	450	–	0.41	2.7
$Ru3/B_2$	139.5	–	0.86	1.1
$Ru20/B_2$	531	–	0.49	2.2
$Cs3.1–Ru3/B_1$	1600	0.96	–	–
$Cs0.33–Ru9.1/B_1$	586	1.76	–	–
$Cs1.59–Ru9.1/B_1$	1150	1.08	–	–
$Cs2.83–Ru20/B_1$	1820	0.96	–	–
$Cs3.03/B_1$	912	0.60	–	–

Further study (Table 3) revealed that the effect of Ru loading on the alkali promoter state is of rather minor importance; an approximate seven-fold increase in ruthenium loading ($Cs3.1–Ru3/B_1$ vs. $Cs2.83–Ru20/B_1$) results in a small (about 20%) enhancement in the Cs reduction degree. Using carbon B_2 instead of B_1 generally leads (see Table 3) to an increase in Cs reduction degree, regardless of the promoter content and ruthenium content. This might be ascribed to the higher BET surface area of carbon B_2 (1257 m^2/g) compared with B_1 (1034 m^2/g), rather than to the differences in Ru dispersion.

In the absence of ruthenium, caesium nitrate deposited on carbon (sample $Cs3.03/B_1$) is also decomposed partly to a form that reacts with water vapour (see Table 3). In that case, however, hydrogen emission and, correspondingly, the Cs reduction degree determined after standard activation (430 °C, 16 h), are considerably smaller (by a factor of 4) than those for the

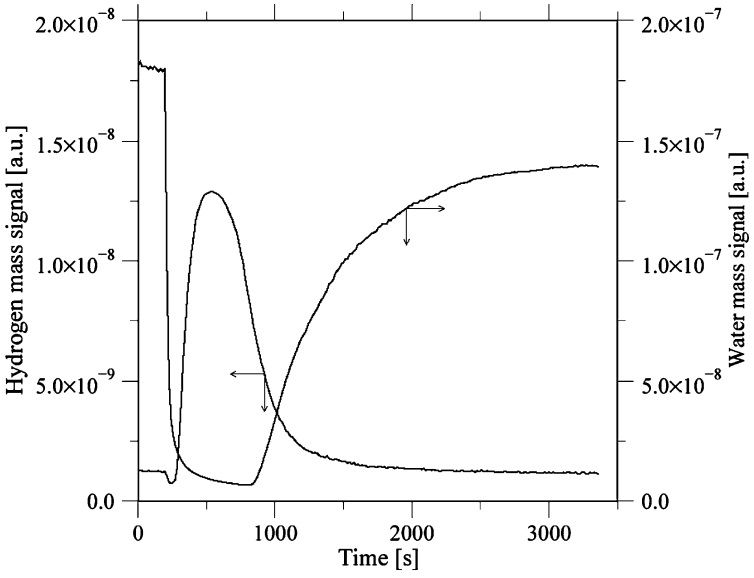

Fig. 7. Interaction of water vapour with the reduced catalyst material. The MS signals of H_2 and H_2O vs. time of the experiment for the $Cs2.64–Ru9.1/B_1$ sample.

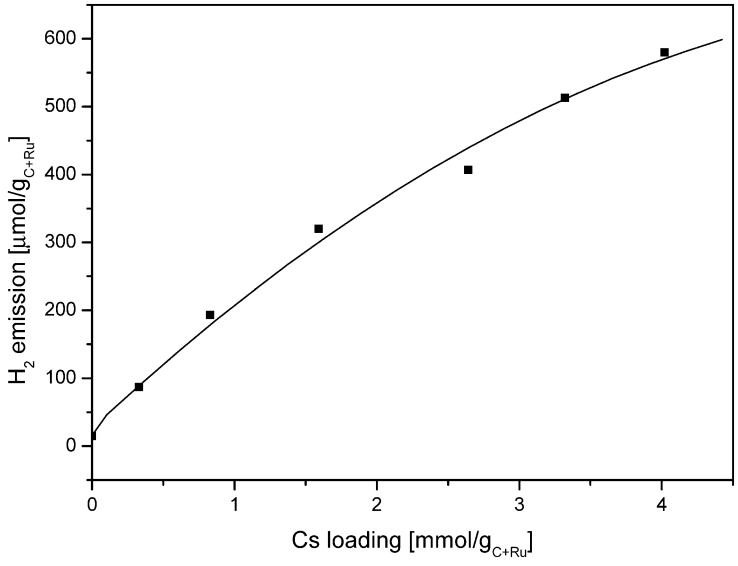

Fig. 8. Interaction of water vapour with the reduced $Cs–Ru9.1/B_1$ catalysts. The hydrogen emission vs. the promoter loading.

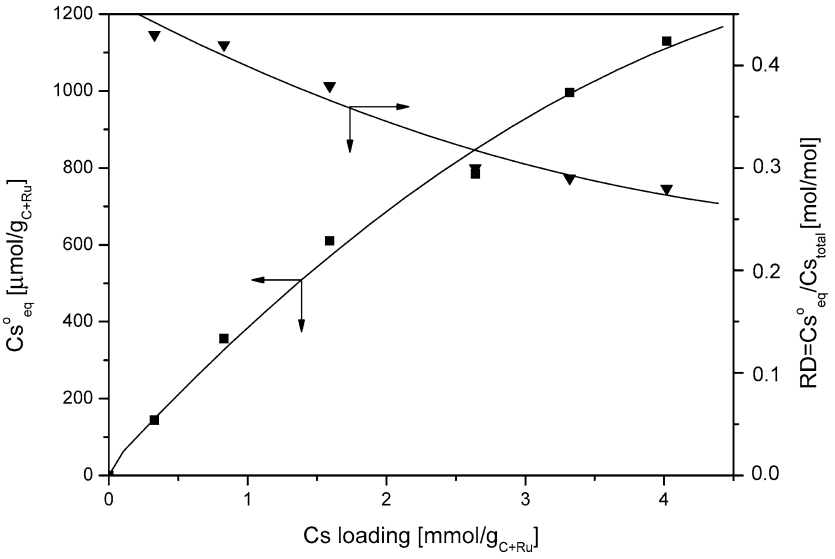

Fig. 9. The number of Cs^0_{eq}. atoms and caesium reduction degree (free RD) vs. the promoter loading in Ru9.1/B_1.

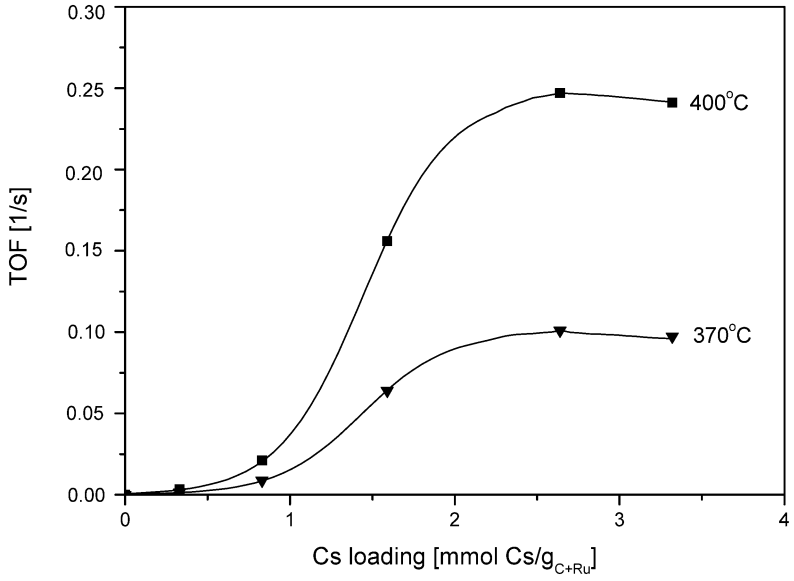

Fig. 10. Integral reaction rate (TOF) of ammonia synthesis vs. caesium content in the Ru9.1/B_1 catalyst; $p = 63$ bar, H_2:$N_2 = 3$:1.

Table 3
Interaction of the reduced Cs–Ru/carbon catalysts with water vapour. Effect of Ru loading and kind of the carbon support

Catalyst	H_2 emission (µmol/g_{C+Ru})	Cs reduction degree (Cs^0_{eq}/Cs_{total}) (mol/mol)
Ru3/B_1	10	–
Cs3.1–Ru3/B_1	412	0.26
Ru9.1/B_1	15	–
Cs3.32–Ru9/B_1	513	0.29
Ru20/B_1	20	–
Cs2.83–Ru20/B_1	480	0.32
Cs3.12–Ru3/B_2	510	0.32
Cs2.57–Ru20/B_2	580	0.43
Cs3.03/B_1 [a]	120	0.079
Cs3.03/B_1 [b]	167	0.11

[a] After standard activation at 430 °C for 16 h.
[b] After activation at 520 °C for 16 h.

Cs–Ru/carbon catalysts of similar Cs loading. Because ruthenium promotes $CsNO_3$ decomposition in H_2, the difference in RD might easily be explained by the kinetic limitation in the decomposition process for the former specimen. Indeed, an increase in activation temperature to 520 °C leads to an RD increase from 0.079 to 0.11, but further treatment of the sample with hydrogen at 550 °C does not change the results. Hence the chemical form (forms) of the promoter in the Cs–Ru/carbon catalyst operating under steady-state NH_3 synthesis conditions seems to be strongly affected by the presence of ruthenium.

3.3. Activity of the catalysts in ammonia synthesis

All the kinetic tests were performed with the catalysts deposited on the same B_1 support. Fig. 10 illustrates the effect of caesium loading in Ru9.1/B_1 on the integral reaction rate (an in-

Table 4
Effect of Ru loading on the integral NH_3 synthesis rate at 63 bar

Catalyst symbol	Ru content in (Ru + supp.) (wt%)	400 °C		370 °C	
		r (g_{NH_3}/(g_{Ru} h))	TOF (1/s)	r (g_{NH_3}/(g_{Ru} h))	TOF (1/s)
Cs3.1–Ru3/B_1	3	73	0.165	29	0.066
Cs2.64–Ru9.1/B_1	9.1	88.5	0.247	36	0.101
Cs2.83–Ru20/B_1	20	68.5	0.275	30	0.121
Cs–Ru/MgO[a]	3.75	23.3	0.060	–	–

[a] Taken from [67].

let H_2:N_2 = 3:1 mixture was free from NH_3) expressed in terms of TOF. To avoid thermodynamic limitations that could influence the relationship, high space velocities were applied in the experiments, thus resulting in small conversions—significantly smaller than those in equilibrium. As shown in Fig. 10, the activity depends strongly on the amount of the promoter introduced. Over the range of small Cs content, up to about 0.9 mmol/g_{C+Ru}, the integral reaction rate (TOF_{int}) increases very slowly. Above this value, TOF_{int} increases dramatically, finally reaching a flat maximum. The optimal Cs loading (2.5–3 $mmol_{Cs}/g_{C+Ru}$) is independent of temperature, and apparent energy of activation ($E_{370–400}$ = 107 kJ/mol) is roughly independent of the promoter amount. A strong effect of Cs loading on the NH_3 synthesis rate is also observed at high ammonia partial pressures in the gas phase. At 8% NH_3 in the $H_2 + N_2$ mixture, the catalyst labelled Cs0.83–Ru9.1/B_1 is approximately an order of magnitude less active (differential rates were determined) than the optimally promoted system (Cs2.64–Ru9.1/B_1) even though the Cs content in the former was only three times less.

Table 4 presents the kinetic data obtained for the Cs–Ru/B_1 systems with different Ru loadings and thus metal dispersions. The surfaces of extra-fine crystallites (1.3 nm) were found to be less active than those of larger crystallites. This finding is in full agreement with our recent results [56] that can be summarised as follows: In the scale of small particles (<4 nm), the surface-based ammonia synthesis rate over Cs–Ru/carbon increases with particle diameter (structure sensitivity of the reaction).

4. Discussion

It is evident that the decomposition of caesium nitrate deposited onto the surface of a Ru/carbon system proceeds via CsOH formation when the material is activated in hydrogen. This was shown experimentally (in situ XRD) for one of the specimens ($CsNO_3$–Ru/A; see Fig. 1). Reduction of NO_3^- anions (caesium nitrate) leads to the sudden evolution of large amounts of H_2O (see Figs. 3 and 4) and thereby to high water vapour concentrations in the gas, thus favouring CsOH, in accordance with thermodynamic calculations in the literature [68]. In the case of $CsNO_3$–Ru/B_1, the alkali precursor is also converted to hydroxide, which remains undetectable by XRD due to high dispersion (extremely small CsOH particles or adsorbed species) forced by the large surface area of carbon B_1. Questions arise, however, as to the steady-state form of caesium (i.e., the form on prolonged activation), as well as the location of the promoter during operation. We discuss these two questions in more detail.

Studies of interaction between water vapour and the Cs–Ru/carbon materials demonstrate that caesium is "partly reduced" after long-term activation. This means that the catalyst surface is covered with the Cs^0 atoms (responsible for H_2 evolution) and also with caesium hydroxide (inert to H_2O), which supplements the alkali balance, or, alternatively, that the surface is decorated solely by substoichiometric oxide, which may also generate H_2 in reaction with water ($Cs_xO_y + (x-y)H_2O = xCsOH + (1/2x-y)H_2$; $x/y > 2$). Clearly, the RD parameter represents either a fraction of Cs^0 atoms in (Cs^0 + CsOH) or reflects an (x/y) stoichiometry in Cs_xO_y, and it is impossible to distinguish between these two options based on the H_2 emission data.

The results of pulse experiments performed with oxygen seem to be helpful in explaining the problem under consideration (Cs^0 + CsOH vs. Cs_xO_y). For the Ru/carbon catalysts with high caesium loading, the O:Cs values (typically 1:1; see Table 2) are about three times higher than those of RD (about 0.3; see Fig. 9 and Table 3). Thus, the differences are too great to justify the concept of Cs^0 atoms coexisting with CsOH on the surface (Cs^0 + CsOH option), even assuming that all of the Cs^0 atoms are transformed to CsO_2 in the pulse experiments. Even then, the experimentally determined O:Cs ratios would be significantly larger (by a factor of 1.7) than those predicted for that option (O:Cs = 0.6:1 is expected for RD = 0.3). In the case of low alkali loading (sample Cs0.33–Ru9.1/B_1), the comparison between O:Cs (1.76:1) and RD (0.43) gives a more decisive response. Whereas the oxidation of Cs^0 atoms to CsO_2 requires only 0.86 mol_O/mol_{Cs}, the oxidation of Cs_xO_y species (Cs_xO_y option; x/y = 3.5 for RD = 0.43) requires 1.72 mol_O/mol_{Cs}, the latter value being in perfect agreement with that determined experimentally. This is a strong evidence that caesium coadsorbed with oxygen (Cs_xO_y species) dominates the catalyst surface when operating. The contribution of CsOH to the caesium balance, if any, seems to be negligible.

The location of the promoter is a separate question. Simple calculations show that caesium introduced to the Ru/carbon system in optimal amounts (2.5–3 mmol/g_{C+Ru} for Ru/B_1) would cover the ruthenium crystallites with several Cs_xO_y layers if located solely on the active metal surface. However, studies of ammonia synthesis over polycrystalline iron foil have revealed that the optimal coverage with potassium is 10–15% [77], and a similar value might be expected for Ru. It is clear, therefore, that an essential part of the total promoter amount must be located on carbon during operation. The other, significantly smaller, part of caesium covers the ruthenium particles. The distribution of Cs_xO_y species between the carbon surface and surface of ruthenium and, consequently, the activating effect of the alkali (with promotion proceeding via direct electron transfer from the alkali to the active metal surface) seem to be controlled by the loading-dependent variations in the heats of alkali adsorption on ruthenium and on carbon, respectively. Support for this supposition comes from studies of alkali adsorption demonstrating that the heat of metallic cae-

sium adsorption on activated carbon ($\Delta H_{Cs/C}$) is very sensitive to coverage [78]. Although at low coverages the alkali metal is very strongly adsorbed on carbon (with $\Delta H_{Cs/C}$ reaching 500 kJ/mol), the heat of adsorption decreases dramatically with increased Cs loading.

Extrapolation of the foregoing results to the region of Cs_xO_y–Ru/carbon systems leads to the conclusion that the trend of TOF versus Cs loading illustrated in Fig. 10 reflects that of Ru coverage by the Cs_xO_y species. Due to the very high heat of adsorption at low caesium content, the Cs_xO_y groups decorate predominantly carbon, whereas the Ru crystallites remain almost uncovered. As a result, a very small promotional effect is observed (see the left part of Fig. 10), even with a high reduction degree of the promoter. As the heat of Cs_xO_y adsorption on carbon falls below a certain value (controlled by the Cs loading), the ruthenium coverage by Cs_xO_y starts to increase dramatically, resulting in a dramatic increase in TOF (see the middle part of Fig. 10; the scope of 0.9–2 $mmol_{Cs}/g_{C+Ru}$). Finally, the Ru coverage by the Cs_xO_y species reaches an optimal value, a full promotional effect (see the right part of Fig. 10).

According to the foregoing considerations, the effect of caesium is determined by the state of the promoter and its location (Ru vs. carbon surfaces), both of which are controlled by the carbon properties from one side and caesium loading from the other side. A strongly reduced form of caesium would be responsible for the significantly higher activities of the optimally promoted Cs–Ru/C catalysts (see Table 4) compared with those of Cs–Ru/MgO, even if the x/y stoichiometries for the Cs_xO_y species located on ruthenium and on carbon were not identical.

5. Conclusion

Ruthenium promotes the decomposition of caesium nitrate deposited onto the surface of Ru/C catalysts when heating the specimens in a hydrogen-containing stream. In the presence of Ru, an onset of the NO_3^- anion reduction (T_{onset}) is shifted (by about 300 °C) toward lower temperatures. $CsNO_3$ is first converted to $CsOH{\cdot}H_2O$, an intermediate product, which is then transformed to a reduced Cs form (reduction degree of 0.25–0.45) or, more specifically, to substoichiometric oxide (Cs_xO_y; $x/y = 2.7$–3.6) covering the catalyst surface under steady-state ammonia synthesis conditions. The distribution of the Cs_xO_y species between the carbon and ruthenium surfaces, along with the x/y stoichiometry in the operating system, are both controlled by the carbon properties and promoter loading. High activities of the optimally promoted Cs–Ru/C catalysts (optimally covered Ru particles by the Cs_xO_y species) are attributed to the strong electron donation (electronic promotion) from the alkali to the active metal surface.

Acknowledgments

This work was carried out under Research Project PBZ-KBN-116/T09/2004 of the Polish Committee for Scientific Research. Z. Kowalczyk, W. Raróg-Pilecka, and E. Miśkiewicz thank the Foundation for Polish Science for financial support.

References

[1] A. Nielsen, An Investigation on Promoted Iron Catalysts for the Synthesis of Ammonia, third ed., Jul. Gielleroups Forlag, Copenhagen, 1968.
[2] Z. Kowalczyk, S. Jodzis, Appl. Catal. A 58 (1990) 29.
[3] J. Schuetze, W. Mahdi, B. Herzog, R. Schloegl, Top. Catal. 1 (1994) 195.
[4] Z. Kowalczyk, Catal. Lett. 37 (1996) 173.
[5] H.Z. Liu, X.N. Li, Chin. J. Catal. 26 (2005) 79.
[6] N. Pernicone, E. Ferrero, I. Rossetti, L. Forni, P. Canton, P. Riello, G. Fagherazzi, M. Signoretto, F. Pinna, Appl. Catal. A 251 (2003) 121.
[7] M.J. Figurski, W. Arabczyk, Z. Lendzion-Blelun, S. Lenart, Appl. Catal. A 266 (2004) 11.
[8] A. Boisen, S. Dahl, C.J.H. Jacobsen, J. Catal. 208 (2002) 180.
[9] C.J.H. Jacobsen, S. Dahl, B.S. Clausen, S. Bahn, A. Logadottir, J.K. Norskov, J. Am. Chem. Soc. 123 (2001) 8404.
[10] C.J.H. Jacobsen, Chem. Commun. (2000) 1057.
[11] R. Kojima, K. Aika, Chem. Lett. (2000) 514.
[12] R. Kojima, K. Aika, Appl. Catal. A 218 (2001) 121.
[13] R. Kojima, K. Aika, Appl. Catal. A 219 (2001) 157.
[14] S. Hagen, R. Barfod, R. Fehrmann, C.J.H. Jacobsen, H.T. Teunissen, K. Stahl, I. Chorkendorff, Chem. Commun. (2002) 1206.
[15] S. Hagen, R. Barfod, R. Fehrmann, C.J.H. Jacobsen, H.T. Teunissen, K. Stahl, I. Chorkendorff, J. Catal. 214 (2003) 327.
[16] F. Rosowski, O. Hinrichsen, M. Muhler, G. Ertl, Catal. Lett. 36 (1996) 229.
[17] O. Hinrichsen, F. Rosowski, A. Hornung, M. Muhler, G. Ertl, J. Catal. 165 (1997) 33.
[18] F. Rosowski, A. Hornung, O. Hinrichsen, D. Herein, M. Muhler, G. Ertl, Appl. Catal. A 151 (1997) 443.
[19] H. Bielawa, O. Hinrichsen, A. Birkner, M. Muhler, Angew. Chem. Int. Ed. 40/6 (2001) 1061.
[20] B.C. McClaine, R.J. Davis, J. Catal. 210 (2002) 387.
[21] S.E. Siporin, R.J. Davis, J. Catal. 225 (2004) 359.
[22] S.E. Siporin, R.J. Davis, J. Catal. 222 (2004) 315.
[23] S.E. Siporin, B.C. McClaine, S.L. Anderson, R.J. Davis, Catal. Lett. 81 (2002) 265.
[24] B.C. McClaine, S.E. Siporin, R.J. Davis, J. Phys. Chem. B 105 (2001) 7525.
[25] B.C. McClaine, R.J. Davis, J. Catal. 211 (2002) 379.
[26] K. Aika, H. Hori, A. Ozaki, J. Catal. 27 (1972) 424.
[27] K. Aika, K. Shimazaki, Y. Hattori, A. Ohya, S. Ohshima, K. Shirota, A. Ozaki, J. Catal. 92 (1985) 296.
[28] S. Murata, K. Aika, J. Catal. 136 (1992) 118.
[29] S. Murata, K. Aika, J. Catal. 136 (1992) 110.
[30] B. Fastrup, Catal. Lett. 48 (1997) 111.
[31] C.J.H. Jacobsen, S. Dahl, P.L. Hansen, E. Tornqvist, L. Jansen, H. Topsøe, D.V. Prip, P.B. Moenshaug, I. Chorkendorff, J. Mol. Catal. A: Chem. 163 (2000) 19.
[32] S. Dahl, J. Sehested, C.J.H. Jacobsen, E. Tornqvist, I. Chorkendorff, J. Catal. 192 (2000) 391.
[33] T.W. Hansen, P.L. Hansen, S. Dahl, C.J.H. Jacobsen, Catal. Lett. 84 (2002) 7.
[34] T.W. Hansen, J.B. Wagner, P.L. Hansen, S. Dahl, H. Topsøe, C.J.H. Jacobsen, Science 294 (2001) 1508.
[35] C.J.H. Jacobsen, J. Catal. 200 (2001) 1.
[36] L. Forni, D. Molinari, I. Rossetti, N. Pernicone, Appl. Catal. A 185 (1999) 269.
[37] I. Rossetti, N. Pernicone, L. Forni, Appl. Catal. A 208 (2001) 271.
[38] Z. Kowalczyk, J. Sentek, S. Jodzis, E. Mizera, J. Góralski, T. Paryjczak, R. Diduszko, Catal. Lett. 45 (1997) 65.
[39] Z. Kowalczyk, S. Jodzis, W. Raróg, J. Zieliński, J. Pielaszek, A. Presz, Appl. Catal. A 184 (1999) 95.
[40] Z. Kowalczyk, S. Jodzis, W. Raróg, J. Zieliński, J. Pielaszek, Appl. Catal. A 173 (1998) 153.
[41] S.E. Siporin, R.J. Davis, W. Raróg-Pilecka, D. Szmigiel, Z. Kowalczyk, Catal. Lett. 93 (2004) 61.
[42] Ch. Liang, Z. Wei, Q. Xin, C. Li, Appl. Catal. A 208 (2001) 193.
[43] X.L. Zhenh, S.J. Zhang, J. Xu, K.M. Wei, Carbon 40 (2002) 2597.

[44] Ch. Liang, Z. Li, J. Qiu, C. Li, J. Catal. 211 (2002) 278.
[45] H.S. Zeng, K. Inazu, K. Aika, Appl. Catal. A 219 (2001) 235.
[46] Z. Zhong, K. Aika, J. Catal. 173 (1998) 535.
[47] Z. Zhong, K. Aika, Inorg. Chem. Acta 280 (1998) 183.
[48] S.M. Yunusov, E.S. Kalyuzhnaya, B.L. Moroz, S.N. Agafonova, V.A. Likholobov, V.B. Shur, J. Mol. Catal. A: Chem. 165 (2001) 141.
[49] Z. Li, Ch. Liang, Z. Feng, P. Ying, D. Wang, C. Li, J. Mol. Catal. A: Chem. 211 (2004) 103.
[50] S. Wu, X.F. Zheng, J.X. Chen, H.S. Zeng, N.J. Guan, Catal. Commun. 5 (2004) 639.
[51] Ch. Liang, Z. Wei, Q. Xin, C. Li, React. Kinet. Catal. Lett. 83 (2004) 39.
[52] A.S. Ivanova, E.S. Kalyuzhnaya, G.S. Litvak, E.A. Moroz, S.M. Yunusov, V.S. Lenenko, B.L. Moroz, V.B. Shur, V.A. Likholobov, Kinet. Catal. 45 (2004) 541.
[53] R.B. Strait, Nitrogen Methanol 238 (1999) 37.
[54] R.B. Strait, S.A. Knez, in: International Conference Exhibition, Caracas, 28 February–2 March 1999.
[55] Z. Kowalczyk, M. Krukowski, W. Raróg-Pilecka, D. Szmigiel, J. Zieliński, Appl. Catal. A 248 (2003) 67.
[56] W. Raróg-Pilecka, E. Miśkiewicz, D. Szmigiel, Z. Kowalczyk, J. Catal. 231 (2005) 11.
[57] W. Raróg, Z. Kowalczyk, J. Sentek, D. Składanowski, J. Zieliński, Catal. Lett. 68 (2000) 163.
[58] G. Ertl, S.B. Lee, M. Weiss, Surf. Sci. 114 (1982) 527.
[59] G. Ertl, in: J.R. Jennings (Ed.), Catalytic Ammonia Synthesis: Fundamentals and Practice, Plenum Press, New York, 1991, p. 109.
[60] J.J. Mortensen, B. Hammer, J.K. Norskov, Phys. Rev. Lett. 80 (1998) 4333.
[61] J.K. Norskov, S. Holloway, N.D. Lang, Surf. Sci. 114 (1984) 65.
[62] D.R. Strongin, G.A. Somorjai, J. Catal. 109 (1988) 51.
[63] D.R. Strongin, G.A. Somorjai, in: J.R. Jennings (Ed.), Catalytic Ammonia Synthesis: Fundamentals and Practice, Plenum Press, New York, 1991, p. 133.
[64] P. Stolze, J.K. Norskov, Top. Catal. 1 (1994) 253.
[65] B. Fastrup, Top. Catal. 1 (1994) 273.
[66] S. Dahl, A. Logadottir, C.J.H. Jacobsen, J.K. Norskov, Appl. Catal. A 222 (2001) 19.
[67] D. Szmigiel, H. Bielawa, M. Kurtz, O. Hinrichsen, M. Muhler, W. Raróg, S. Jodzis, Z. Kowalczyk, L. Znak, J. Zieliński, J. Catal. 205 (2002) 205.
[68] S.R. Tennison, in: J.R. Jennings (Ed.), Catalytic Ammonia Synthesis: Fundamentals and Practice, Plenum Press, New York, 1991, p. 303.
[69] M. Guraya, S. Sprenger, W. Raróg-Pilecka, D. Szmigiel, Z. Kowalczyk, M. Muhler, Appl. Surf. Sci. 238 (2004) 77.
[70] N.B. Shitova, M.N. Dobrynkin, A.S. Noskov, I.P. Prosvirin, V.I. Bukhtiyarov, D.I. Kochubei, P.G. Tsyrulnikov, D.A. Shlyapin, Kinet. Catal. 45 (2004) 414.
[71] H.S. Zeng, K. Inazu, K. Aika, J. Catal. 211 (2002) 33.
[72] S. Wu, C.M. Zheng, J.X. Chen, X.F. Zheng, H.S. Zeng, N.J. Guan, Chin. J. Catal. 25 (2004) 873.
[73] I. Rossetti, N. Pernicone, L. Forni, Appl. Catal. A 248 (2003) 97.
[74] Z. Kowalczyk, J. Sentek, S. Jodzis, R. Diduszko, A. Presz, A. Terzyk, Z. Kucharski, J. Suwalski, Carbon 34 (1996) 403.
[75] Z. Kaszkur, J. Appl. Crystallogr. 33 (2000) 1262.
[76] K. Aika, T. Takano, S. Murata, J. Catal. 136 (1992) 126.
[77] E. Tornqvist, A.A. Chen, Catal. Lett. 8 (1991) 359.
[78] E.E. Anderson, G.L. Wessman, L.R. Zumwalt, Nucl. Sci. Eng. 12 (1962) 106.